Prepared for submission to JINST

11TH International Conference on Position Sensitive Detectors
3RD-8TH September 2017
The Open University, Milton Keynes, UK

# Characterization of Irradiated APDs for Picosecond Time Measurements

**M. Centis Vignali,**[a,1] **R. Dalal,**[b] **M. Gallinaro,**[a,c] **B. Harrop,**[d] **G. Jain,**[b] **C. Lu,**[d] **M. McClish,**[e] **K. T. McDonald,**[d] **M. Moll,**[a] **F. M. Newcomer,**[f] **S. Otero Ugobono,**[a,g] **S. White**[a,h]

[a] *CERN, Geneva, Switzerland*
[b] *University of Delhi, Delhi, India*
[c] *LIP, Lisbon, Portugal*
[d] *Princeton University, Princeton, USA*
[e] *Radiation Monitoring Devices, Watertown, USA*
[f] *University of Pennsylvania, Philadelphia, USA*
[g] *Universidade de Santiago de Compostela, Santiago de Compostela, Spain*
[h] *University of Virginia, Charlottesville, USA*

*E-mail:* matteo.centis.vignali@cern.ch

Abstract: For their operation at the CERN High Luminosity Large Hadron Collider (HL-LHC), the ATLAS and CMS experiments are planning to implement dedicated systems to measure the time of arrival of minimum ionizing particles with an accuracy of about 30 ps. The timing detectors will be subjected to radiation levels corresponding up to a 1-MeV neutrons fluence ($\Phi_{eq}$) of $10^{15}$ cm$^{-2}$ for the goal integrated luminosity of HL-LHC of 3000 fb$^{-1}$.

In this paper deep-diffused Avalanche Photo Diodes (APDs) produced by Radiation Monitoring Devices are examined as candidate timing detectors for HL-LHC applications. These APDs are operated at 1.8 kV, resulting in a gain of up to 500. The timing performance of the detectors is evaluated using a pulsed laser. The effects of radiation damage on current, signal amplitude, noise, and timing of the APDs are evaluated using detectors irradiated with neutrons up to $\Phi_{eq} = 10^{15}$ cm$^{-2}$.

Keywords: Timing detectors, Solid state detectors, Radiation-hard detectors

[1] Corresponding author.

## Contents



## 1 Introduction

The high luminosity upgrade of the CERN Large Hadron Collider (HL-LHC) foreseen to start in 2026 will provide an instantaneous luminosity of $5 \cdot 10^{34}\,\mathrm{cm}^{-2}\mathrm{s}^{-1}$ with a bunch spacing of 25 ns, and an average pile-up of 200 collisions per bunch crossing. To reduce the effects of pile-up on the physics analyses, both the ATLAS and CMS experiments are planning to implement dedicated systems to measure the time of arrival of minimum ionizing particles (MIPs) with an accuracy of about 30 ps. These systems include both scintillators coupled to photo-detectors and silicon detectors. By providing the time of arrival information of MIPs, these systems allow for the correct association of particles to their primary vertexes in the case where the latter have a proximity in space that renders their separation impossible. An improved time of arrival resolution would also effectively reduce the vertex density, and improve the vertex reconstruction capability of the experiments. These timing detectors will be subjected to radiation levels corresponding to a 1-MeV neutrons fluence ($\Phi_{eq}$) of up to $10^{15}\,\mathrm{cm}^{-2}$ for the goal integrated luminosity of HL-LHC of $3000\,\mathrm{fb}^{-1}$.

This paper summarizes the characterization of neutron irradiated Avalanche Photo Diodes (APDs) produced by Radiation Monitoring Devices (RMD) [1]. Studies of these sensors as MIP timing detectors were performed previously and showed promising results [2]. The sensors under study and their irradiation are described in section 2. Section 3 presents the experimental methods used in this work. Section 4 and 5 show the results obtained for the current-voltage characteristic and signal amplitude of the samples. Finally, section 6 contains the results relevant for the time resolution of the sensors under study.

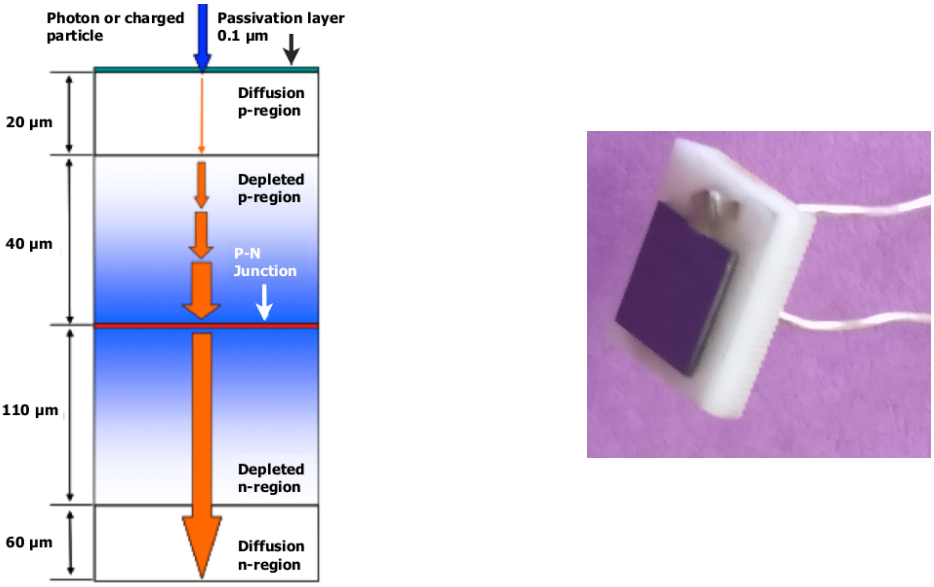


**Figure 1**. **Left:** Schematic cross-section of a deep-diffused APD. **Right:** Picture of one of the devices used in this study. The APD is packaged on a ceramic support.

## 2 Deep-Diffused Avalanche Photo Diodes

The APDs used in this work are produced using the method explained in [3, 4]. A schematic cross-section and a picture of the resulting device are shown in figure 1. The APDs consist of a pn-junction operated in reverse bias. The applied bias is around 1.8 kV, resulting in a region in the detector where the field is high enough for the charge carriers to undergo impact ionization. This mechanism is responsible for the multiplication of the charge carriers released by the passage of a charged particle. The gain of the detector at 1.8 kV is around 500. The doping profile ensures that the depletion region does not reach the top and bottom surfaces of the detector. This allows to apply to the detector bias voltages in the kV range. The detectors used in this work have an active area of $2 \times 2\,\mathrm{mm}^2$.

The sensors were irradiated with neutrons at the nuclear reactor of the Jožef Stefan Institute in Ljubljana [5]. The fluences accumulated by the sensors ranged from $\Phi_{eq} = 3 \cdot 10^{13}\,\mathrm{cm}^{-2}$ to $\Phi_{eq} = 10^{15}\,\mathrm{cm}^{-2}$. Neither bias nor cooling were applied during the irradiation. After irradiation, the samples were stored at a temperature below $-18°\mathrm{C}$ to avoid the annealing of the defects produced during irradiation.

## 3 Experimental Methods

Two experimental setups were used to characterize the APDs. In order to facilitate the handling and electrical connection to the sensors, each packaged APD (see figure 1) was mounted on a printed circuit board (PCB) for its characterization. The PCB was equipped with a temperature sensor and the connectors needed to link the APD to the measuring devices.

The current-voltage characteristic of the detectors was measured using a voltage source and a picoammeter connected in series to the sensor under test. The sensor was placed inside a climate

chamber flushed with dry air where the temperature could be controlled. The temperature sensor on the PCB was used to ensure that the APD reached thermal equilibrium with the air in the climate chamber before starting the measurements.

The response of the APDs to a pulsed infrared laser was measured in a different setup and used to determine the variation of the sensor's signal and time resolution as a function of bias voltage and irradiation fluence. The laser has a wavelength of 1064 nm and the pulses have a duration of 200 ps. The repetition rate was chosen to be 200 Hz. The intensity of the light impinging on the APD was determined to correspond to a charge deposition in the sensor of 15 MIPs per pulse. The amount of deposited charge per laser pulse was measured using a non-irradiated pad diode of known thickness. The wavelength used has an absorption length in silicon of about 1 mm, resulting in the generation of electron hole pairs through the whole sensor thickness. The light pulses are propagated from the laser to the sensor through an optical fiber. A coupler diverts part of the light to a photodiode that is used to monitor the intensity of the light pulses. An optical system focuses the light on the sensor surface producing a beam spot of about 15 $\mu$m in diameter. The bias voltage of the sensor under test is provided by a voltage source containing a picoammeter used to monitor the current flowing through the sensor. The temperature of the APD was controlled using a cooling system constituted by a Peltier element and a chiller. The temperature measured by the temperature sensor on the PCB was used as input to the Peltier control system. The APD was housed in a light-tight Faraday cage flushed with dry air during the measurements. The APD signal was amplified using a CIVIDEC C2HV broadband amplifier [6]. Both the signals of the APD and the photodiode were digitized using an oscilloscope.

For the measurement of the APD signal amplitude, an amplification of 10 dB was used. This amplification was achieved by attenuating the APD signal with a 30 dB attenuator and then amplifying it with a 40 dB amplifier. The 40 dB amplifier is the same used in the time resolution measurements. The reduction of the gain to 10 dB is necessary in order to perform the amplitude measurements over the desired bias voltage range while remaining in the amplifier's linear range. For each measurement condition, the waveforms were averaged 256 times in the oscilloscope before being stored for analysis.

The time resolution measurements were performed applying a 40 dB amplification to both the APD and the photodiode signal. No averaging was applied to the waveforms. A gain of 40 dB provides a better signal to noise ratio for the APD signal, compared to the 10 dB used for the amplitude measurement. The amplified photodiode signal, for the given light intensity, provides a reference for the time measurement with a resolution of $\sigma_t = 4.2 \pm 0.1$ ps. Since the intensity of the light shining on the photodiode is proportional to the one of the light shining on the APD, in order to maintain the time resolution of the photodiode signal, the light shining on the APD was constrained to have an intensity corresponding to 15 MIPs per pulse.

The APD temperature was $-20^{\circ}$C during all measurements reported in this paper. For all the measurements using the laser, the light was shone on the center of the APDs.

## 4 Current-Voltage Characteristic

The current-voltage (IV) characteristic of the APDs is shown, for different fluences, in figure 2. Before irradiation, below 1600 V, the current assumes a value of less than a few nA. In this region

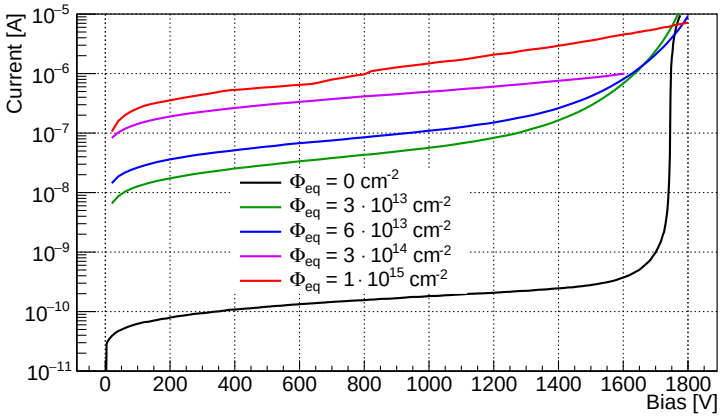


**Figure 2**. Current-voltage characteristics of the APDs measured at −20°C for different fluences.

the main contribution to the current is thought to be surface current. Between 1600 and 1800 V, the current increases by 4 orders of magnitude. This is the region where the multiplication dominates the IV characteristic of the non-irradiated sensors. The surface current is not affected by multiplication, therefore the multiplication of bulk current in the non-irradiated sensors can not be seen in the IV curve until the gain is sufficiently high.

The irradiation enhances the bulk generation current of the devices, as can be seen in the region between 0 and 1200 V, where the gain of the sensors does not influence the curves. As the bulk current is amplified, the shape of the irradiated sensors' curves is different from that of the non-irradiated sensor. The change in the magnitude of the current at high voltages is different with respect to the non-irradiated sensor, suggesting that the gain of the detectors is reduced by irradiation, or respectively that a higher bias voltage is required to obtain the same gain as for the non-irradiated sensor.

The sensor irradiated to $\Phi_{eq} = 3 \cdot 10^{14}\,\mathrm{cm}^{-2}$ shows a breakdown around 1600 V, therefore no information about its IV characteristic is available at higher bias voltages. This also applies to the amplitude measurements presented in the next section.

## 5 Signal Amplitude

The amplitude of the APD signal was measured using the laser setup described in section 3. The amplitude was measured from the baseline of the pulse, calculated using the part of the waveform preceding the laser pulse. The results are shown in figure 3 as a function of bias voltage and fluence.

The measured amplitudes present similar values up to 1200 V, for all the fluences. For voltage values above 1200 V, the signal amplitude decreases with increasing fluence, indicating a reduction of the gain for the irradiated detectors.

## 6 Time Resolution

The time resolution measurements were performed using the laser setup described in section 3. The main differences with respect to the setup used for the amplitude measurements are the different

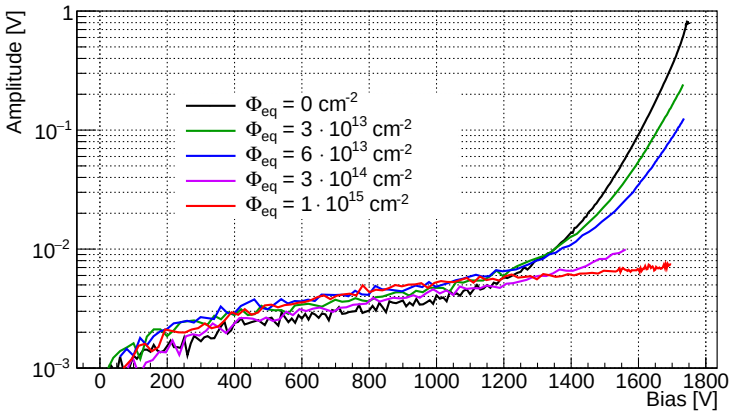


**Figure 3**. Amplitude of the APDs signal as a function of bias voltage and fluence measured at −20°C. The laser intensity corresponds to 15 MIPs. An amplification of 10 dB was used.

signal amplification, the amplification of the photodiode signal, and the fact that the waveforms were not averaged in the scope. For each measurement condition, 1500 waveforms were acquired. The sensor irradiated to $\Phi_{eq} = 3 \cdot 10^{14}\,\mathrm{cm}^{-2}$ was not used in the measurements presented in this section due to its breakdown behavior.

During these measurements it was noticed that the sensor irradiated to $\Phi_{eq} = 10^{15}\,\mathrm{cm}^{-2}$ presents some "dark pulses" with an amplitude corresponding to several MIPs. These pulses are randomly occurring and are not related to the laser illumination, ruling out effects similar to the after-pulse of silicon photomultipliers as an explanation for their presence. The frequency at which "dark pulses" with an amplitude above a threshold of 30 mV occur was found to be around 3 MHz for the highest bias voltage applied to the sensor. The "dark pulses" influence the measurements presented in this section. The events where "dark pulses" with an amplitude exceeding 30 mV precede the signal from the laser pulse were excluded from the data analysis. For each bias configuration, less than 75 out of the 1500 waveforms were excluded.

The average amplitude of the pulses is shown in figure 4. The measurements were constrained by the amplifier, that allows a maximum output amplitude of about 1 V. This translates in different bias voltages applied to the sensors. The sensors irradiated up to $\Phi_{eq} = 6 \cdot 10^{13}\,\mathrm{cm}^{-2}$ show a signal amplitude similar to the non-irradiated one, although at higher bias voltages. The voltage applied to the sensor irradiated to $\Phi_{eq} = 10^{15}\,\mathrm{cm}^{-2}$ is not sufficient to achieve the same amplitude as the other sensors. The maximum applicable bias voltage was limited by other setup components other than the amplifier.

The noise is defined as the standard deviation of the distribution of the waveform points around the baseline, for the portion of the waveform preceding the pulse due to laser illumination. The noise of the APDs, as a function of bias voltage and irradiation fluence, is shown in figure 5. The noise of the APDs with $\Phi_{eq} \leq 6 \cdot 10^{13}\,\mathrm{cm}^{-2}$ shows a strong dependence on the applied bias voltage. The voltage at which the noise exceeds 5 mV corresponds to a signal amplitude of roughly 0.6 V for these sensors, suggesting that the multiplication mechanism is responsible for the increase in the noise. If the contribution of the "dark pulses" to the noise distribution were to be included, the

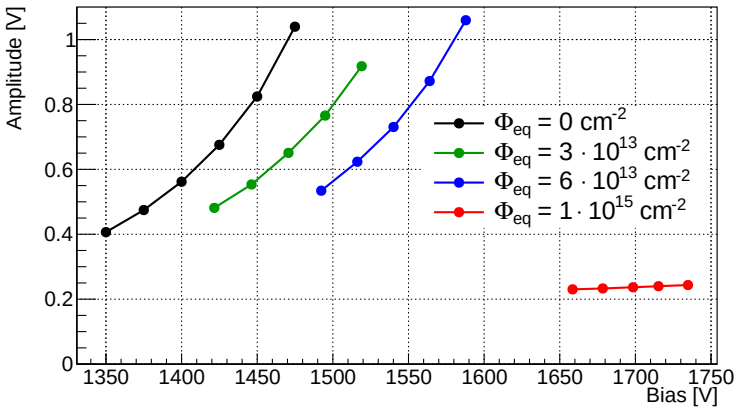


**Figure 4**. Average amplitude of the APDs signal as a function of bias voltage and fluence measured at −20°C. The laser intensity corresponds to 15 MIPs. An amplification of 40 dB was used.

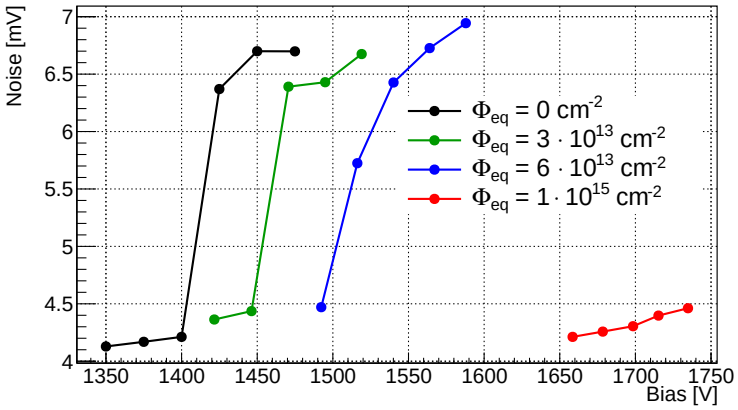


**Figure 5**. APDs' noise as a function of bias voltage and fluence measured at −20°C. An amplification of 40 dB was used.

noise of the sensor irradiated to $\Phi_{eq} = 10^{15}$ cm$^{-2}$ would lie between 5 and 6 mV. For the calculation of the signal to noise ratio reported below, the values of noise shown in figure 5 were used.

The signal to noise ratio (SNR) is defined as the ratio between amplitude and noise and is shown in figure 6.

The average 20%-to-80% rise time of the sensors is shown in figure 7. The crossing time of the 20% and 80% thresholds was determined using a linear interpolation between two points of the waveform. The rise time does not seem to be much affected by irradiation. The difference between the rise time of the sensors lies within 6% and is probably due to tolerances in the sensor production.

The time resolution of the overall system consisting of APD and photodiode (*system APD-photodiode*) is shown in figure 8 as a function of bias voltage and fluence. The time resolution is defined as the standard deviation of the distribution of the time difference ($\Delta t$) between the APD and the photodiode signal. The algorithm used to determine the signal timing is a constant fraction discriminator (CFD) implemented in software. The CFD thresholds were optimized for

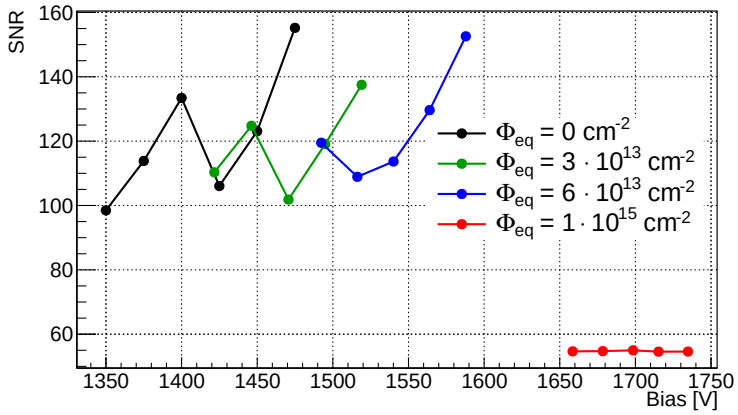


**Figure 6**. Signal to noise ratio of the APDs as a function of bias voltage and fluence measured at −20°C. The laser intensity corresponds to 15 MIPs. An amplification of 40 dB was used.

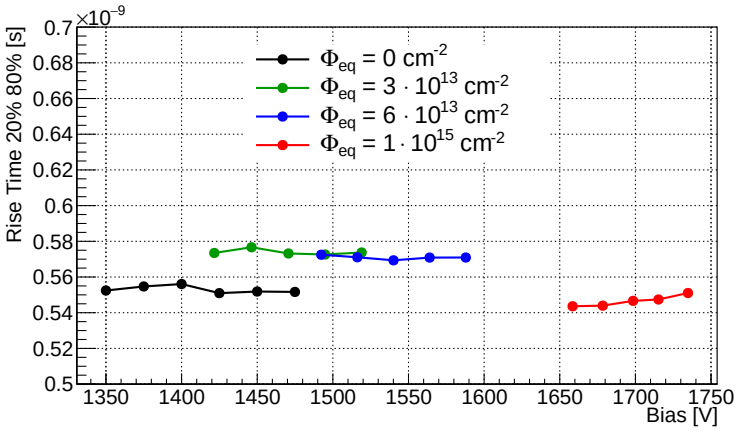


**Figure 7**. 20%-to-80% rise time of the APDs as a function of bias voltage and irradiation fluence measured at −20°C. The laser intensity corresponds to 15 MIPs. An amplification of 40 dB was used.

each measurement condition. The crossing time of the CFD thresholds was determined using a linear interpolation between two points of the waveform. The time resolution of the system is similar for the sensors with $\Phi_{eq} \leq 6 \cdot 10^{13}\,\mathrm{cm}^{-2}$. The best result for a light intensity of 15 MIPs was obtained using the non-irradiated sensor yielding $\sigma_{\Delta t} = 6.7 \pm 0.1$ ps, corresponding to a time resolution of the APD $\sigma_t = 5.2 \pm 0.2$ ps after the resolution of the time reference is subtracted. By including the events with "dark pulses" in the analysis, the time resolution of the sensor irradiated to $\Phi_{eq} = 10^{15}\,\mathrm{cm}^{-2}$ would worsen by about 2 ps. The CFD thresholds were set higher than the "dark pulses" amplitude during the optimization process.

The time resolution was found to be a function of the APDs' SNR, as shown in figure 9. The time resolution scales roughly with 1/SNR; this behavior is represented by a dashed line. As the SNR is affected by the measurement setup, an improvement of the readout electronics can result in an improvement in the time resolution, for both non-irradiated and irradiates sensors.

The time resolution of the APDs is not degraded by neutron irradiation up a fluence of at least

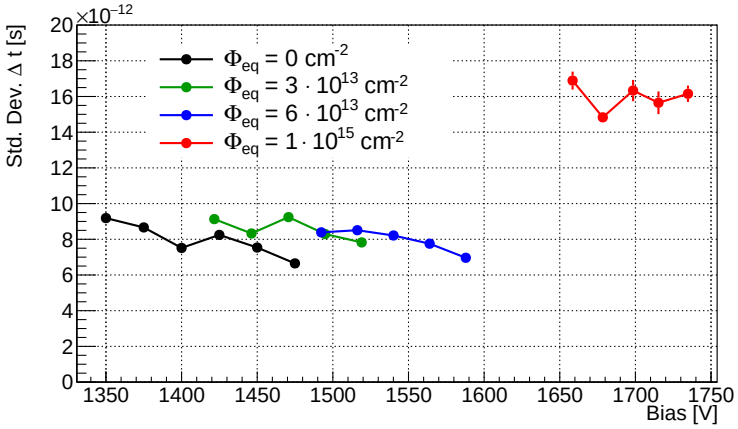


**Figure 8**. Time resolution of the *system APD-photodiode* as a function of bias voltage and fluence measured at −20°C. The laser intensity corresponds to 15 MIPs. An amplification of 40 dB was used.

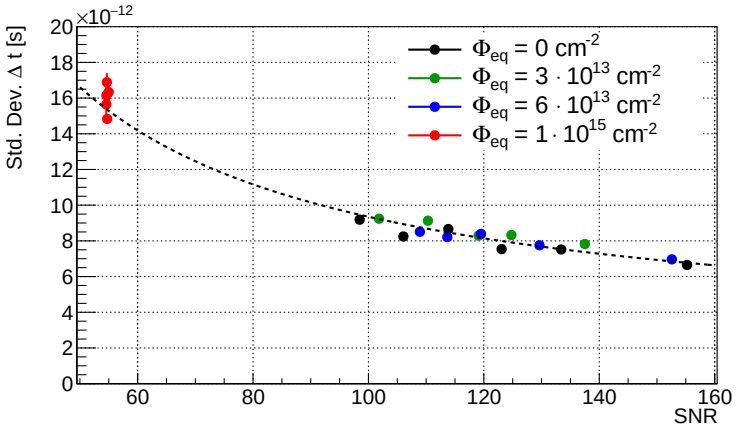


**Figure 9**. Time resolution of the *system APD-photodiode* as a function of the APD signal to noise ratio measured at −20°C. The laser intensity corresponds to 15 MIPs. An amplification of 40 dB was used. The time resolution scales roughly with 1/SNR, represented by a dashed line.

$\Phi_{eq} = 6 \cdot 10^{13}\,\mathrm{cm}^{-2}$.

Due to the constraints of the measurement setup, the light intensity used in these measurements corresponds to 15 MIPs. This did not allow to perform measurements through the full range of bias voltage and gain of the devices. The possibility of increasing the gain of the devices has to be taken into account if the results shown in this paper were to be scaled for a lower charge deposited in the sensor. The expected charge deposition in a HL-LHC application is 1 MIP and follows the distribution derived in [7]. Results obtained with non-irradiated sensors using a light intensity corresponding to 1 MIP are shown in [2]. The study of the timing performance of the APDs presented in this paper is foreseen to be repeated using a light intensity corresponding to 1 MIP.

In the measurements presented in this section a CFD algorithm was used to estimate the timing performance of the detectors. The algorithm was chosen due to its versatility in exploring the

different thresholds for each measurement condition, and therefore signal amplitude. In the case of timing measurements with charged particles, the CFD is necessary to correct the time walk resulting from the distribution of the energy deposit in the sensor. As long as the shape of the signal remains constant, although with different amplitude, the CFD is expected to provide an effective time walk correction. An effect that cannot be corrected by the CFD and can constitute a significant deviation of the timing performance of the sensors between laser pulses and charged particles, is the variation of the amount of charge deposited per unit length along the particle path. These fluctuations, also known as *Landau noise* [8], can influence the leading edge of the sensor's signal and therefore worsen the time resolution. These effects must be studied in dedicated beam tests. A comparison of the timing performance obtained with laser pulses and in beam tests will help to quantify how these fluctuation affect the APDs' timing performance.

## 7 Summary

Deep-diffused APDs with an active area of $2 \times 2\,\mathrm{mm}^2$ produced by RMD were irradiated with reactor neutrons up to a fluence of $\Phi_{eq} = 10^{15}\,\mathrm{cm}^{-2}$. Current, amplitude, and timing characteristics of the detectors were measured at a temperature of $-20°\mathrm{C}$ before and after irradiation.

From the current-voltage characteristic it was found that the bulk current of the detectors increases with irradiation and that the gain decreases with irradiation. The latter observation is supported by measurements of the APDs signal performed using a pulsed infrared laser.

The time resolution of the APDs was determined using a pulsed infrared laser with an intensity corresponding to 15 MIPs per pulse. The time resolution is not degraded by exposure to fluences of up to at least $\Phi_{eq} = 6 \cdot 10^{13}\,\mathrm{cm}^{-2}$.

The device irradiated to $\Phi_{eq} = 10^{15}\,\mathrm{cm}^{-2}$ shows the presence of "dark pulses" with a frequency of around 3 MHz and an amplitude corresponding to several MIPs.

The study of these devices will continue through beam tests and improvements of the measurement setup.

These devices, with their current design, could be used as timing detectors in parts of the HL-LHC experiments where the fluences are in a range up to about $\Phi_{eq} = 10^{14}\,\mathrm{cm}^{-2}$, with the upper bound to be studied with more detail than presented in this paper.

## Acknowledgments

The work summarized in this paper has been performed within the framework of the RD50 collaboration. This project has received funding from the European Union's Horizon 2020 Research and Innovation programme under Grant Agreement no. 654168.

## References

[1] Radiation Monitoring Devices Inc., 44 Hunt St. Watertown USA, http://rmdinc.com/

[2] S. White, *R&D for a Dedicated Fast Timing Layer in the CMS Endcap Upgrade*, Acta Physica Polonica B Proceedings Supplement No. 4 Vol. 7 (2014).

[3] R. Farrell, K. Vanderpuye, *Large area semiconductor detector with internal gain*, US Patent 7,268,339.

[4] M. McClish et al., *Characterization of very large silicon avalanche photodiodes*, IEEE Symposium Conference Record Nuclear Science 2004, pp. 1270-1273 Vol. 2.

[5] L. Snoj, G. Žerovnik, A. Trkov, *Computational analysis of irradiation facilities at the JSI TRIGA reactor*, Applied Radiation and Isotopes, Volume 70, Issue 3, 2012.

[6] CIVIDEC Instrumentation GmbH, Schottengasse 3A Wien Austria, http://cividec.at/

[7] H. Bichsel, *Straggling in thin silicon detectors*, Rev. Mod. Phys., Volume 60, Issue 3, 1988.

[8] N. Cartiglia et al., *Tracking in 4 dimensions*, NIM A, Volume 845, 2017.